

The Impact of Best Track Discrepancies on Global Tropical Cyclone Climatologies using IBTrACS

CARL J. SCHRECK III

Cooperative Institute for Climate and Satellites–North Carolina, North Carolina State University, and NOAA/National Climatic Data Center, Asheville, North Carolina

KENNETH R. KNAPP AND JAMES P. KOSSIN

NOAA/National Climatic Data Center, Asheville, North Carolina

(Manuscript received 14 January 2014, in final form 18 June 2014)

ABSTRACT

Using the International Best Track Archive for Climate Stewardship (IBTrACS), the climatology of tropical cyclones is compared between two global best track datasets: 1) the World Meteorological Organization (WMO) subset of IBTrACS (IBTrACS-WMO) and 2) a combination of data from the National Hurricane Center and the Joint Typhoon Warning Center (NHC+JTWC). Comparing the climatologies between IBTrACS-WMO and NHC+JTWC highlights some of the heterogeneities inherent in these datasets for the period of global satellite coverage 1981–2010. The results demonstrate the sensitivity of these climatologies to the choice of best track dataset. Previous studies have examined best track heterogeneities in individual regions, usually the North Atlantic and west Pacific. This study puts those regional issues into their global context. The differences between NHC+JTWC and IBTrACS-WMO are greatest in the west Pacific, where the strongest storms are substantially weaker in IBTrACS-WMO. These disparities strongly affect the global measures of tropical cyclone activity because 30% of the world's tropical cyclones form in the west Pacific. Because JTWC employs similar procedures throughout most of the globe, the comparisons in this study highlight differences between WMO agencies. For example, NHC+JTWC has more 96-kt ($\sim 49 \text{ m s}^{-1}$) storms than IBTrACS-WMO in the west Pacific but fewer in the Australian region. This discrepancy probably points to differing operational procedures between the WMO agencies in the two regions. Without better documentation of historical analysis procedures, the only way to remedy these heterogeneities will be through systematic reanalysis.

1. Introduction

Tropical cyclones are among the world's most destructive natural disasters (Rappaport 2000; Webster 2008; Smith and Katz 2013). As such, they have become a focal point in society's concerns over the changing climate (Pielke et al. 2005; Emanuel 2005; Webster et al. 2005; Seneviratne et al. 2012; Christensen et al. 2014; Hartmann et al. 2014). Observational studies of tropical cyclones and climate change rely on so-called “best track” datasets, which nominally provide estimates of the tropical cyclone locations and intensities. Forecast

centers generate these data in real time as part of their warning cycle, and most agencies reevaluate them at the end of the season with the benefit of hindsight and more complete data. Unfortunately, changes in operational procedures and observing capabilities through time and between agencies have introduced heterogeneities into the best track data (Hagen and Landsea 2012; Vecchi and Knutson 2008; Landsea et al. 2010; Knapp and Kruk 2010; Kossin et al. 2013). These changes limit our ability to know if and how climate change has affected tropical cyclones (Wu et al. 2006; Knutson et al. 2010; Seneviratne et al. 2012; Christensen et al. 2014; Hartmann et al. 2014).

The International Best Track Archive for Climate Stewardship (IBTrACS; Knapp et al. 2010) collects many diverse best track datasets from forecast centers and historical archives into a single compendium. Having these datasets in a single format promotes comparisons

Corresponding author address: Carl J. Schreck III, Cooperative Institute for Climate and Satellites–NC, 151 Patton Ave., Asheville, NC 28801.
E-mail: cjschrec@ncsu.edu

between them, which can be valuable for identifying and quantifying their heterogeneities (Knapp and Kruk 2010; Song et al. 2010; Knapp et al. 2013).

Knapp and Kruk (2010) identified linear relationships between the wind data from agencies around the globe with IBTrACS. They found that many of these relationships changed with time, exacerbating the challenge of reconciling these datasets. Other studies have examined how the best track heterogeneities have affected the climatology and trend analysis of tropical cyclones in individual regions, particularly the North Atlantic (Landsea 2007; Mann et al. 2007; Vecchi and Knutson 2008; Landsea et al. 2010) and west Pacific (Kamahori et al. 2006; Yu et al. 2007; Nakazawa and Hoshino 2009; Song et al. 2010; Ren et al. 2011; Barcikowska et al. 2012; Knapp et al. 2013). Kossin et al. (2007, 2013) examined temporal heterogeneities in the best track dataset by comparing data from a single agency in each region with reanalyses based on homogenized satellite data (Knapp et al. 2011).

None of these previous studies examined the differences between best track datasets on a global scale. The current study fills that gap by comparing the climatology of tropical cyclones using two global datasets derived from IBTrACS:

- 1) IBTrACS-WMO, the recently introduced World Meteorological Organization (WMO) subset of IBTrACS, which uses data from the official WMO agency in each region, and
- 2) NHC+JTWC, a combination of data from two U.S. agencies: the National Oceanic and Atmospheric Administration's (NOAA) National Hurricane Center (NHC) for the North Atlantic and east Pacific and the military's Joint Typhoon Warning Center (JTWC) for the remainder of the globe.

One benefit of this methodology is that JTWC applies similar procedures in all regions since the 1987 termination of aircraft reconnaissance in the west Pacific. Comparisons between NHC+JTWC and IBTrACS-WMO in various regions can shed light on differences between nonoverlapping WMO agencies. This study will demonstrate how these variations between best track sources can affect global climatologies of tropical cyclones.

2. Heterogeneities in tropical cyclone maximum winds

One key source of heterogeneity in the historical records of tropical cyclones is the definition of their maximum winds. The WMO standard for tropical cyclones is the maximum 10-min sustained wind within a storm at 10 m over a smooth surface, something rarely observed. However, agencies in the United States use

a 1-min wind, and Regional Specialized Meteorological Center (RSMC) New Delhi reports a 3-min wind. In addition to these differences in wind averaging period, the methods for deriving those winds have also changed with time and between agencies.

Most regions lack the benefit of aircraft reconnaissance and instead rely on satellite estimates of wind speed from the Dvorak technique (Dvorak 1972, 1973, 1975, 1984; Velden et al. 2006a,b). This quasi-objective technique enables analysts to derive a current intensity (CI) number based on satellite imagery. The CI number is then converted to a wind speed or central pressure through a lookup table. The Dvorak technique was developed in the United States, so the original table lists 1-min winds. Agencies in other countries often modify this table to convert the winds to another averaging period or to adjust for local tropical cyclone characteristics (Koba et al. 1990, 1991; Harper et al. 2010; Knapp and Kruk 2010). The most common modification is multiplying the 1-min winds by 0.88 to roughly convert to 10-min values. RSMC Tokyo, on the other hand, uses a completely unique table (Koba et al. 1989, 1990, 1991). This table was derived based on matching their best track data during the reconnaissance era with reanalyzed CI numbers. The Koba et al. (1990, 1991) table increases the winds for low CI numbers and decreases them for high CI numbers (Nakazawa and Hoshino 2009; Knapp and Kruk 2010; Barcikowska et al. 2012).

Converting best track winds to CI numbers has been proposed as one method for homogenizing the data between agencies, but large differences still remain (Nakazawa and Hoshino 2009; Knapp and Kruk 2010; Barcikowska et al. 2012). For example, RSMC New Delhi reports 3-min winds that are a factor of 0.77 smaller than the 1-min winds from JTWC (Knapp and Kruk 2010). However, comparing RSMC New Delhi's best track wind speeds with their CI numbers suggest that they use the original 1-min tables (Knapp and Kruk 2010). The only explanation is that the CI numbers derived by RSMC New Delhi are significantly lower than those from JTWC, so these CI numbers cannot be used to reconcile the deviations between these agencies.

Similar issues have been found in the west Pacific between JTWC and RSMC Tokyo. Nakazawa and Hoshino (2009) compared operational CI numbers between the two agencies. Meanwhile, Barcikowska et al. (2012) converted the RSMC Tokyo best track winds to CI numbers with the Koba et al. (1990, 1991) table. These in turn were converted back to 1-min winds through the Dvorak (1984) table. In both studies, JTWC still had significantly higher winds than RSMC Tokyo, especially for stronger storms in the 1990s. There are several possible explanations for these remaining differences:

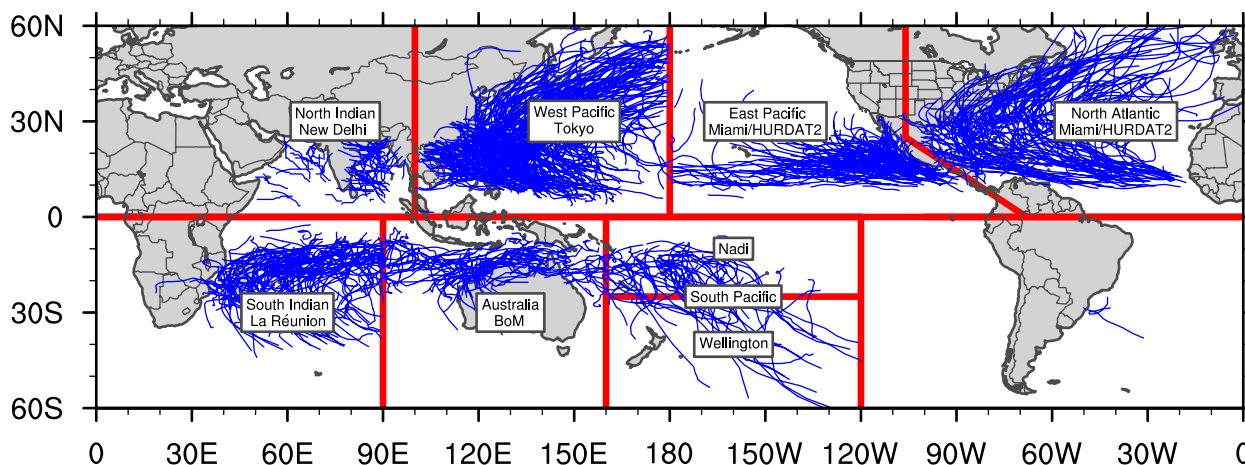


FIG. 1. Regions and data sources for this study overlaid with tropical cyclone (≥ 35 kt) tracks for 2000–10.

- The agencies might have placed differing emphasis on supplementary data like surface observations and microwave satellite retrievals (Barcikowska et al. 2012).
- Some aspects of the Dvorak analysis are subjective and can result in disagreements of 0.5 CI number from one analyst to another (Knaff et al. 2010; Torn and Snyder 2012; Landsea and Franklin 2013). While this error is small in a Dvorak CI number sense, it can translate into wind speed deviation of up to 15 kt ($1 \text{ kt} = 0.5144 \text{ m s}^{-1}$) for the strongest storms (Knaff et al. 2010).
- In addition to the CI-to-wind tables, the Dvorak technique includes several rules that constrain how quickly the CI number can change through the life of a storm. The application of these rules is known to vary from one agency to another, which can impact the maximum strength that a storm achieves (Velden et al. 2006b; Nakazawa and Hoshino 2009; Knaff et al. 2010).

Given these diverse sources of heterogeneity and their temporal variability, it is unlikely that the best track datasets can be reconciled without manual reanalysis.

Rather than seeking to homogenize the data, this study will simply compare the global climatologies derived from the original IBTrACS-WMO and NHC+JTWC datasets. Such a comparison will inform future studies on how the selection of one dataset or the other might affect their results. To facilitate this comparison, the only change we have made to the data is to approximate a 1-min wind by simply dividing all winds from RSMCs Tokyo, Fiji, Wellington, La Réunion, and the Australian Bureau of Meteorology (BoM) by 0.88. The data from RSMCs Miami and New Delhi and from NHC+JTWC are used in their original form. Unfortunately, the conversion factor of 0.88 does not fully address the heterogeneities discussed above, but it at least reverses the most common adjustments to the

Dvorak tables, thus making wind speeds more comparable.

Although 1-min winds are not the WMO standard, many previous studies of tropical cyclone activity (e.g., Maue 2009, 2011; Kossin et al. 2007, 2010; Blake and Kimberlain 2013; Avila and Stewart 2013; Diamond 2013) have used 1-min wind data to count storms by their category on the Saffir–Simpson hurricane wind scale (Saffir 1973; Simpson 1974; Schott et al. 2012) or to calculate accumulated cyclone energy (ACE; Bell et al. 2000). Using a 1-min wind here improves our ability to compare with such previous work.

3. Data

All best track data in this study come from IBTrACS v03r05. IBTrACS is the most complete collection of best track datasets currently available. It includes data from all of the WMO RSMCs and tropical cyclone warning centers (TCWCs), JTWC, the Shanghai Typhoon Institute, the Hong Kong Observatory, and several historical archives. Previous versions of IBTrACS, as described by Knapp et al. (2010), averaged these disparate datasets in an attempt to derive a consensus value. The combining of wind speeds via an arithmetic average was discontinued in IBTrACS v03r01 because of input and guidance received from participants at the first IBTrACS Workshop (Levinson et al. 2010) due to heterogeneities in how the data are derived.

IBTrACS now includes the original data from all available best track datasets beginning with v03r01. This compendium is referred to as IBTrACS-All, and it allows direct comparison of the datasets (e.g., Knapp and Kruk 2010; Song et al. 2010; Knapp et al. 2013). For users that simply want a single track and intensity for each storm, IBTrACS now also offers a WMO subset

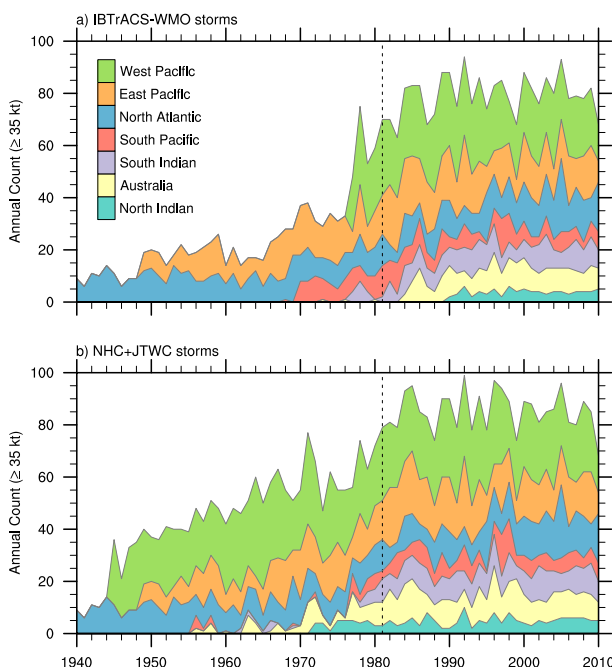


FIG. 2. Tropical cyclones (≥ 35 kt) per year broken down by region for (a) IBTrACS-WMO and (b) NHC+JTWC.

(IBTrACS-WMO). This subset includes only data from the RSMC/TCWC responsible for a given region (Fig. 1). Note that the three TCWCs from the BoM provide a collective best track dataset. Similarly, the data from RSMC Honolulu, which is responsible for the central North Pacific, is included in the second-generation hurricane database (HURDAT2) from RSMC Miami (Landsea and Franklin 2013).

For the purposes of this study, we use a subset of the IBTrACS-All dataset that contains data only from NHC and JTWC (NHC+JTWC). Until the advent of IBTrACS, similar NHC+JTWC datasets, such as the version available from Professor K. Emanuel's web page (<http://eaps4.mit.edu/faculty/Emanuel/products>), were the only options available for global coverage (Lander and Guard 1998; Klotzbach 2006; Frank and Young 2007; Kossin et al. 2007; Maue 2009, 2011). It should be noted that NHC+JTWC is identical to IBTrACS-WMO in the North Atlantic and east Pacific, where NHC/RSMC Miami is the WMO agency.

IBTrACS includes a flag to denote a storm's basin. While the WMO regions (Fig. 1) are used in the creation of IBTrACS-WMO, this basin flag uses somewhat different definitions in the Southern Hemisphere. It omits the Australian region and instead uses 135°E as the dividing line between the South Pacific and the south Indian basins. To contrast BoM with its neighbors, this study will use the WMO-defined regions in Fig. 1 rather than those that are in the IBTrACS dataset.

TABLE 1. Period of record for each region and dataset. The year 1990 appears in bold for the north Indian region, as that is the beginning of global coverage for IBTrACS-WMO.

	NHC+JTWC	IBTrACS-WMO
North Atlantic	1981–2010	1981–2010
East Pacific	1981–2010	1981–2010
West Pacific	1981–2010	1981–2010
North Indian	1981–2010	1990 –2010
South Indian	1980/81–2009/10	1981/82–2009/10
Australia	1980/81–2009/10	1984/85–2009/10
South Pacific	1980/81–2009/10	1980/81–2009/10
Northern Hemisphere	1981–2010	1981–2010
Southern Hemisphere	1980/81–2009/10	1980/81–2009/10
Global	1981–2010	1981–2010

The boundaries between WMO regions can be somewhat arbitrary, and storms occasionally cross them with interesting consequences for the data. For example, when a storm crosses from one region to another, the IBTrACS-WMO data comes from a different RSMC for each portion of the track. Another consequence arises from this study's focus on counting storms that reach various intensity thresholds (35, 64, and 96 kt). In this study, storms are counted based on when and where they first achieve each threshold. That means that a given tropical cyclone may be counted as a 35-kt storm in one basin but a 64-kt storm in another if it crosses a boundary during its intensification. However, storms are never counted more than once for the same threshold.

4. Methods

a. Data to be omitted

IBTrACS collects all available tropical cyclone best track data. This wealth of data means that not all of it is suitable for all applications. For example, sometimes agencies will track completely separate circulations for portions of a storm's life cycle. Because IBTrACS cannot reconcile these large disparities, or "spurs," it breaks them into separate tracks. To identify these tracks, IBTrACS includes a "track type" flag, which can be set to main, merge, split, or other. Spurs occur 109 times in the 1981–2010 period but 458 times in the presatellite era. **For the purposes of counting storms, it is important to only include "main" tracks to avoid double counting.**

Practices for best-tracking storms after extratropical transition vary from one agency to another. Many best track datasets include a form of "nature" flag that specifies whether or not the storm is tropical. In some cases, this flag even gives information about the strength of the storm. With the goal of uniformity, IBTrACS standardizes these flags to tropical, subtropical, extratropical, disturbance, conflicting, not reported, and missing. For

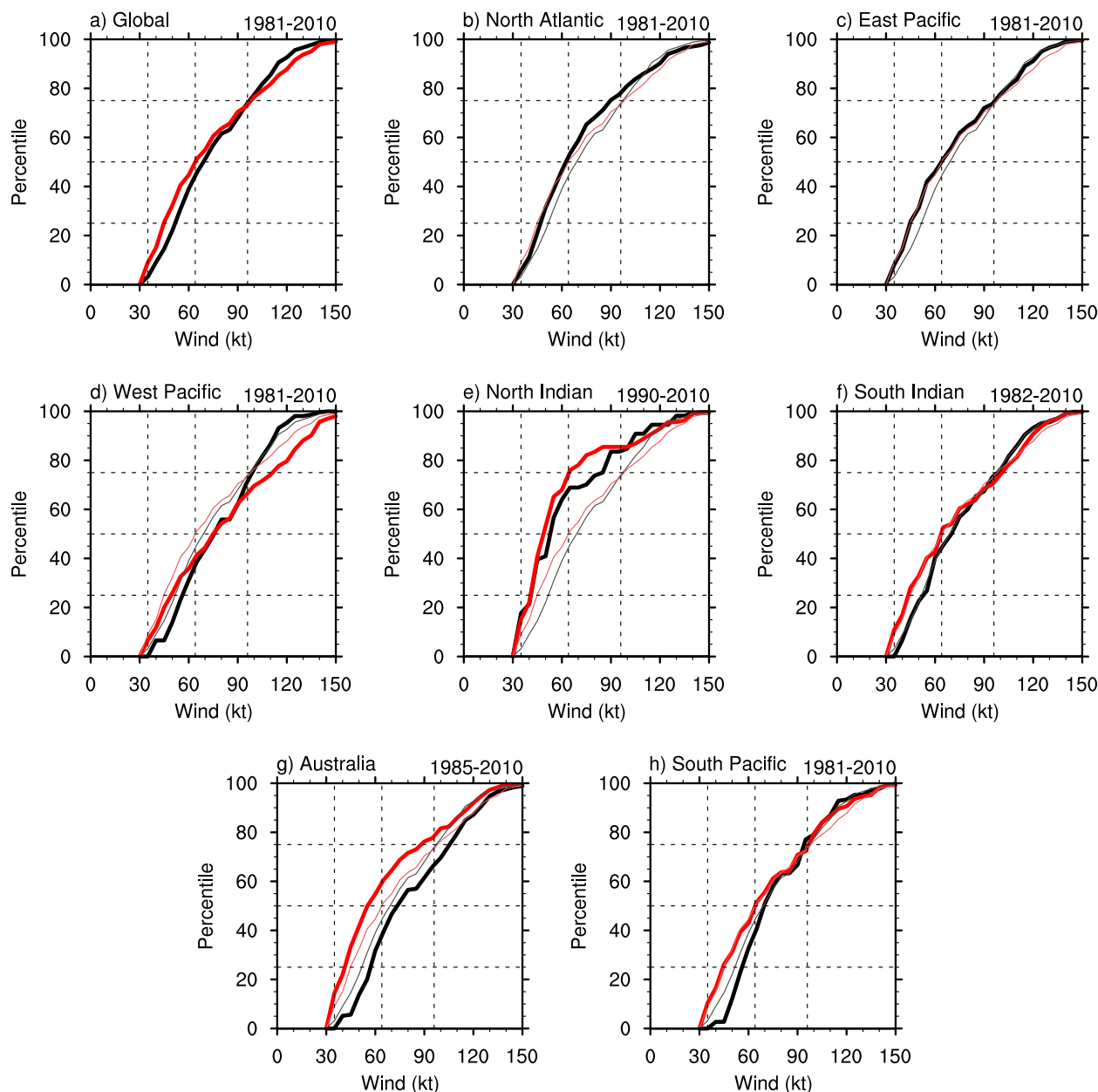


FIG. 3. Cumulative density functions for storm LMI in each region: IBTrACS-WMO (black) and JTWC+NHC (red). Global values are shown as thin lines in each region for reference. Vertical dashed lines identify 35, 64, and 96 kt, while horizontal lines denote quartiles. Years in the upper right denote the period of record for IBTrACS-WMO. NHC+JTWC is 1981–2010 for all regions.

the purposes of this study, we have excluded any observations that are flagged as extratropical or disturbance.

All of the metrics in this study are based on winds, whether they are ACE or counting the number of storms above a given wind threshold. For 1981–2010, IBTrACS-WMO contains 53 out of 2662 tracks that lack wind information, mostly in the Australian region where BoM did not record winds routinely until 1985. These tracks are omitted from the current study.

b. Period of record

No extended period can be considered entirely temporally homogeneous. For example, Landsea et al. (2010) found that ongoing improvements to observation and analysis systems have led to an artificial trend in short-duration (<2 days) storms. Such a spurious trend would affect the annual mean number of 35-kt storms (Villarini et al. 2011), but its

TABLE 2. Percentiles of storm LMI (kt) for each region along with the strongest storms in each dataset from the initial year listed through 2010.

Region	Source	Initial year	50th	75th	90th	95th	Max
North Atlantic	WMO: Miami	1981	65	95	121	130	160
East Pacific	WMO: Miami	1981	65	100	120	125	160
West Pacific	WMO: Tokyo	1981	80	97	114	119	142
West Pacific	JTWC	1981	75	115	135	140	160
North Indian	WMO: New Delhi	1990	55	85	105	120	140
North Indian	JTWC	1981	50	65	115	125	145
South Indian	WMO: La Réunion	1981/82	71	97	114	125	143
South Indian	JTWC	1980/81	65	105	120	130	150
Australia	WMO: BoM	1984/85	75	106	125	129	153
Australia	JTWC	1980/81	58	90	120	128	155
South Pacific	WMO: Nadi/Wellington	1980/81	68	91	114	125	148
South Pacific	JTWC	1980/81	65	100	119	133	155
Global	WMO	1981	70	97	115	125	160
Global	NHC+JTWC	1981	65	100	125	135	160

effects on higher-intensity storms and ACE would be smaller.

Figure 2 shows the number of 35-kt storms per year broken down by region for IBTrACS-WMO (Fig. 2a) and NHC+JTWC (Fig. 2b). The global number of storms in each dataset shows a marked increase over the past 70 years. Closer inspection reveals that much of this increase is due to limited periods of record in some regions. For example, RSMC Tokyo began reporting tropical cyclone tracks in 1951 (not shown), but they did not report winds until 1977. As a result, the global number of 35-kt tropical cyclones in IBTrACS-WMO nearly doubles from 1976 to 1977 (Fig. 2a). In IBTrACS-WMO, the last regions to achieve routine wind observations are the south Indian (1981/82), Australian (1984/85), and north Indian (1990) regions. For NHC+JTWC, the last regions are the South Pacific (1977/78) and the south Indian (1978/79). However, Chu et al. (2002) note that JTWC's data since 1985 are more reliable than earlier years.

Table 1 lists the years that will be used for each region and dataset. This study focuses on 1981–2010 for three primary reasons:

- 1) 1981 approximates the beginning of global coverage in each dataset (Fig. 2);
- 2) this period roughly corresponds with the period of global satellite coverage, which should provide more complete and less heterogeneous data; and
- 3) 1981–2010 corresponds to the latest normals that have been released by NOAA for other geophysical variables (Arguez et al. 2012; Applequist et al. 2012; Durre et al. 2013) and have already been used in the

annual summaries from RSMC Miami (Avila and Stewart 2013; Blake and Kimberlain 2013; Diamond 2013).

Since complete global coverage in IBTrACS-WMO only begins in 1990, some results in this study will be presented for 1990–2010. Either 21 years (1990–2010) or 30 years (1981–2010) should provide robust interannual statistics of tropical cyclones, as it does for other geophysical variables (Arguez and Vose 2011; Arguez et al. 2013). However, known interdecadal oscillations (Kossin and Vimont 2007; Aiyer and Thorncroft 2011) preclude our ability to draw conclusions about long-term trends from these data.

The tropical cyclone seasons will be January–December for the Northern Hemisphere and July–June for the Southern Hemisphere. Most Southern Hemisphere storms occur in January–March (Lander and Guard 1998), so global values will use January–December.

5. Results

a. Lifetime maximum intensity

Figure 3 and Table 2 present the cumulative density functions for storm lifetime maximum intensity (LMI) for tropical cyclones ($\text{LMI} \geq 35$ kt) in each region and dataset. Figure 3 highlights the 64- and 96-kt thresholds, which correspond to category 1 (hurricane) and category 3 (major hurricane) on the Saffir–Simpson hurricane wind scale (Saffir 1973; Simpson 1974; Schott et al. 2012). An interesting coincidence is that these thresholds align closely with the 50th and 75th percentiles

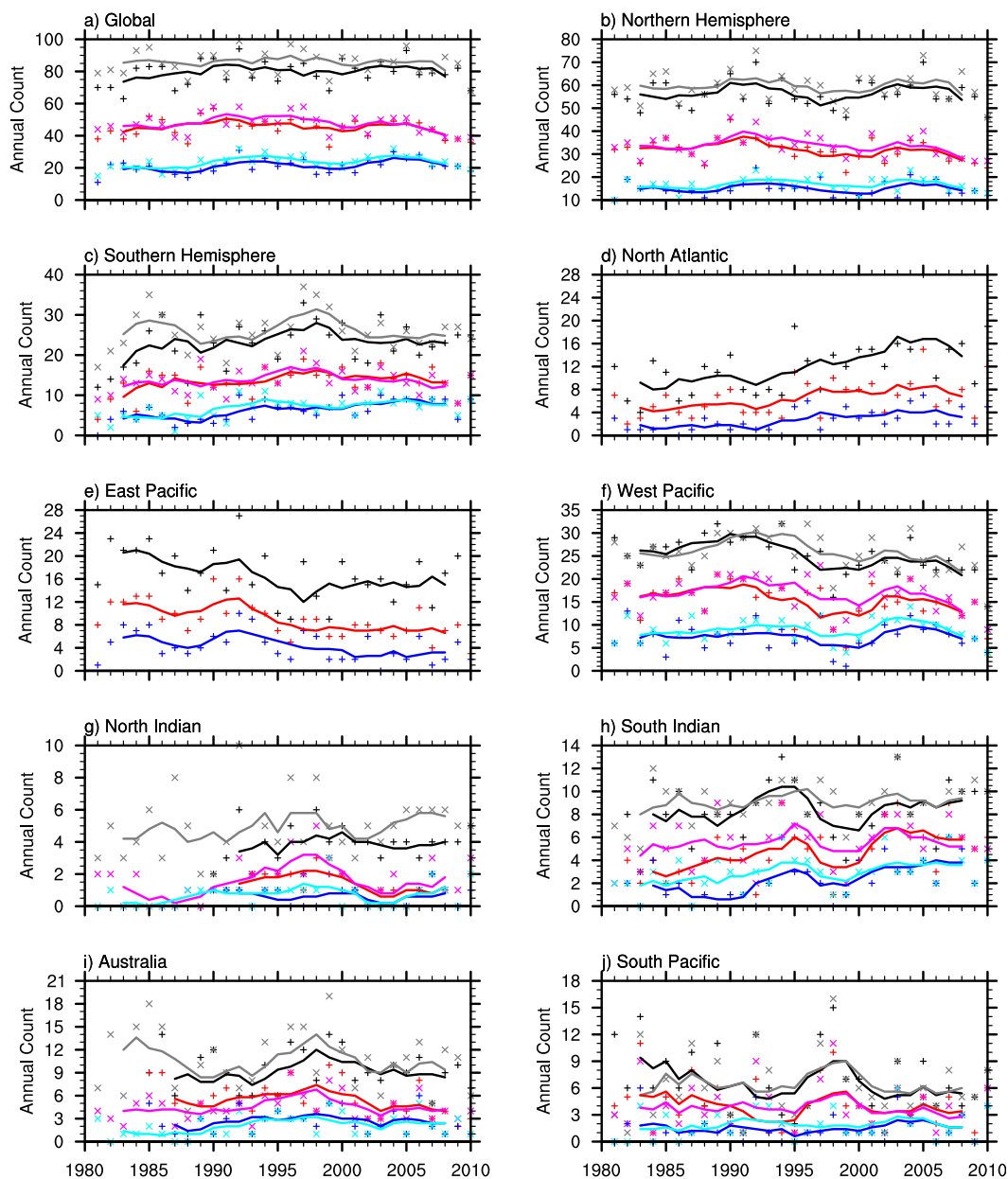


FIG. 4. Annual counts of 35- (black/gray), 64- (red/magenta), and 96-kt (blue/aqua) tropical cyclones for each region using IBTrACS-WMO [black/red/blue lines and cross (+) markers] and NHC+JTWC [gray/magenta/aqua lines and crisscross (×) markers]. Markers are the annual counts, while the lines show 5-yr running averages.

for global LMI. It is unlikely that Saffir and Simpson had this in mind during their development, but it suggests that these thresholds have some physical meaning.

The distributions of LMI (Fig. 3) for most regions (thick lines) are similar to the global distribution (thin lines). The north Indian region is a notable exception, with storms that are much weaker than elsewhere. Median storms in other regions would approach the upper

quartile in the north Indian. These lower intensities could be related in part to the lack of direct geostationary satellite coverage before 1998, which would have hindered Dvorak estimates of intensity (Landsea et al. 2006; Kossin et al. 2013).

Except for the west Pacific and Australia, most regions show reasonable agreement in the LMI distributions between IBTrACS-WMO (Fig. 3, black) and NHC+JTWC (red). In the Australian region, JTWC

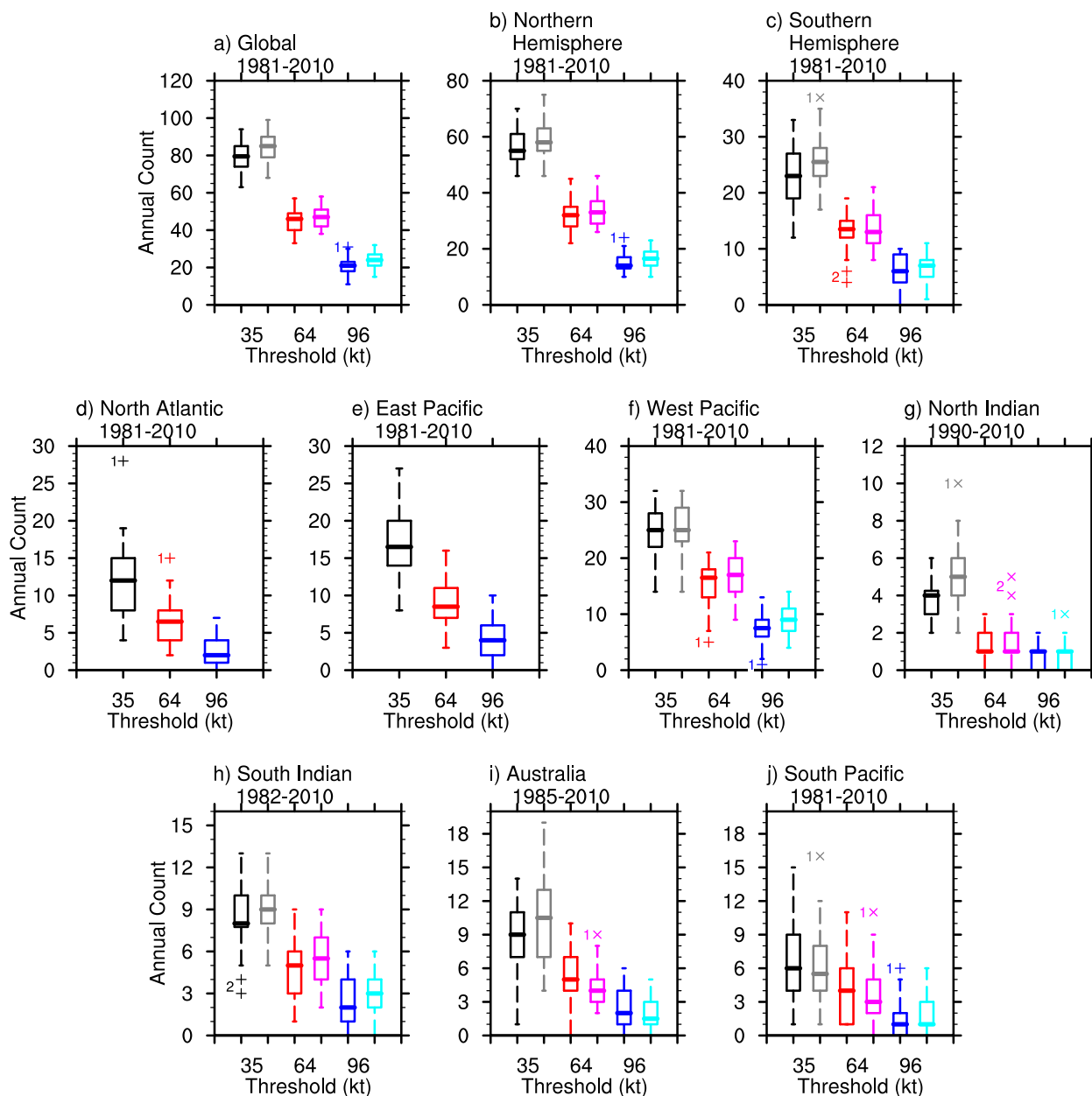


FIG. 5. Box-and-whisker plots of annual counts of 35- (black/gray), 64- (red/magenta), and 96-kt (blue/aqua) tropical cyclones for each region using IBTrACS-WMO (black/red/blue) and NHC+JTWC (gray/magenta/aqua). The heavy line denotes the median, while thin horizontal lines mark upper and lower quartiles. The whiskers extend to the maximum and minimum values, excluding any outliers. Outliers are defined as falling more than 1.5 interquartile ranges from the nearest quartile and are identified with markers and numbers showing how many outliers are near each other. Years at the top denote the period of record for IBTrACS-WMO. NHC+JTWC is 1981–2010 for all regions.

and BoM have similar distributions of LMI for the strongest 10% of storms, but BoM has stronger LMIs for intermediate storms. JTWC and RSMC Tokyo have similar distributions of LMI below 90 kt in the west Pacific. However, they diverge for stronger storms with JTWC reporting higher LMI values. This divergence is symptomatic of the nonlinear relationships between

JTWC and RSMC Tokyo found by previous studies (Nakazawa and Hoshino 2009; Knapp and Kruk 2010; Song et al. 2010; Barcikowska et al. 2012).

The contrast between JTWC and RSMC Tokyo is particularly stark when comparing the storms with the strongest LMI for the 30-yr period (Table 2). JTWC has reported three storms in the past 30 years with

TABLE 3. The 25th, 50th, and 75th percentiles for each region of the annual number of tropical cyclones exceeding 35, 64, and 96 kt. Boldface distributions are significantly greater than the other dataset at the 95% level using the Wilcoxon signed rank test, while italicized distributions are only significantly greater at the 90% level. All data are from the initial year listed through 2010.

Region	Source	Initial year	≥35 kt			≥64 kt			≥96 kt		
			25th	50th	75th	25th	50th	75th	25th	50th	75th
North Atlantic	WMO: Miami	1981	8	12	15	4	6.5	8	1	2	4
East Pacific	WMO: Miami	1981	14	16.5	20	7	8.5	11	2	4	6
West Pacific	WMO: Tokyo	1981	22	25	28	13	16.5	18	6	7.5	9
West Pacific	JTWC	1981	23	25	29	14	17	20	7	9	11
North Indian	WMO: New Delhi	1990	3	4	4.25	1	1	2	0	1	1
North Indian	JTWC	1981	4	5	6	1	1	2	0	1	1
South Indian	WMO: La Réunion	1981/82	7.75	8	10	3	5	6	1	2	4
South Indian	JTWC	1980/81	8	9	10	4	5.5	7	2	3	4
Australia	WMO: BoM	1984/85	7	9	11	4	5	7	1	2	4
Australia	JTWC	1980/81	7	10.5	13	3	4	5	1	1.5	3
South Pacific	WMO: Nadi/Wellington	1980/81	4	6	9	1	4	6	0	1	2
South Pacific	JTWC	1980/81	4	5.5	8	2	3	5	1	1	3
Northern Hemisphere	WMO	1981	52	55	61	28	32	35	13	14	17
Northern Hemisphere	NHC+JTWC	1981	55	58	63	29	33	37	14	16.5	19
Southern Hemisphere	WMO	1980/81	20	22.5	26	12	13	16	4	6.5	8
Southern Hemisphere	JTWC	1980/81	23	25	28	11	13	15	5	7	8
Global	WMO	1981	74	79.5	85	40	46	49	18	21	23
Global	NHC+JTWC	1981	79	85	90	42	47	51	21	24	27
Global	WMO	1990	76	80	86	42.25	46	49	18.75	22	25.25
Global	NHC+JTWC	1990	79.75	86	90.25	41.75	49	51	21	24	27

intensities of 160 kt, while the strongest two storms from RSMC Tokyo had LMIs of only 142 kt. These maximum LMIs are at opposite ends of the spectrum when compared to other regions. The North Atlantic and the east Pacific are the only other regions with storms reaching 160 kt, while only the north Indian region has a weaker maximum than 142 kt.

b. Storms per year

1) GLOBAL AND REGIONAL PATTERNS

Figure 4 shows the annual number of tropical cyclones that reach intensities of at least 35 (black), 64 (red), and 96 kt (blue) for each region. Figure 5 and Table 3 identify the medians and quartiles for these annual counts. These statistics were calculated over the periods listed in Table 1, which do not necessarily match between the two datasets. However, the statistical significance of differences between the datasets was calculated for the common period (i.e., the IBTrACS-WMO period) using the Wilcoxon signed rank test (Wilks 2006, p. 160).

The global number of 35-kt tropical cyclones is 74–85 in IBTrACS-WMO and 79–90 in NHC+JTWC, consistent with other recent studies (Lander and Guard 1998; Frank and Young 2007). NHC+JTWC has significantly more storms globally for all three intensity levels (Table 3, Fig. 5a). The lack of IBTrACS-WMO data in some regions during the 1980s contributes to these differences, particularly in the Southern Hemisphere

(Fig. 4c). Even so, Table 3 shows similar relationships for 1990–2010 when IBTrACS-WMO has full global coverage.

The west Pacific usually has about 22–29 35-kt storms annually in each dataset, but JTWC has significantly more 64- and 96-kt tropical cyclones than RSMC Tokyo (Table 3, Fig. 5f). These discrepancies align with the distribution of LMI (Fig. 3d), which also shows similarities between the two datasets for weaker storms but not for the stronger ones. Figure 4f suggests that the numbers of 64-kt storms diverge in the 1990s and then converge again in the 2000s, consistent with previous studies (Nakazawa and Hoshino 2009; Ren et al. 2011; Barcikowska et al. 2012; Knapp et al. 2013). Several factors may have conspired to produce this deviation: 1) the termination of aircraft reconnaissance in 1987, 2) increasing availability of microwave satellite wind retrievals, and 3) a relaxation of the Dvorak temporal wind constraints at JTWC. Interestingly, the disparity in 96-kt tropical cyclones seems to be more persistent throughout the record.

The north Indian region has significantly more 35-kt tropical cyclones from JTWC than from RSMC New Delhi (Table 3). Although their medians are only one storm apart (five versus four), JTWC has more 35-kt tropical cyclones for 17 of the 21 years for which both datasets are available (Fig. 4g). Similarly, they have identical medians and quartiles for annual 64-kt cyclones (Table 3), but the Wilcoxon signed rank test

TABLE 4. Average number of tropical cyclones (≥ 35 kt) for each region, the percentage of the global total accounted for that region, and the interannual standard deviation. The global mean is defined as the sum of the region means to account for differing periods of record. Boldface values are significantly different between IBTrACS-WMO and NHC+JTWC at the 95% level using a paired t test.

	Avg storms per year				Percent of global total				Std dev (storms)			
	Lander and Guard (1998)		Gray (1968)		Lander and Guard (1998)		Gray (1968)		Lander and Guard (1998)		Gray (1968)	
	IBTrACS-WMO	NHC+JTWC	IBTrACS-WMO	NHC+JTWC	IBTrACS-WMO	NHC+JTWC	IBTrACS-WMO	NHC+JTWC	IBTrACS-WMO	NHC+JTWC	IBTrACS-WMO	NHC+JTWC
North Atlantic	7	9.8	12.1	12.1	11.3	11.5	14.8	14.3	3.4	4.9	4.9	4.9
East Pacific	10	15.8	16.5	16.5	16.1	18.6	20.2	19.4	3.8	4.6	4.6	4.6
West Pacific	22	27.1	25.0	25.7	35.5	31.9	30.6	30.3	4.5	4.2	4.2	4.2
North Indian	8	4.8	3.9	4.9	12.9	5.7	4.8	5.8	2.4	1.2	1.2	1.9
South Indian	6		8.4	9.0	9.7		10.3	10.6		2.4	2.4	1.9
Australia	2		9.1	10.4	3.2		11.1	12.2		3.1	3.1	4
South Pacific	7		6.8	6.3	11.3		8.3	7.4		3.9	3.9	3.5
Northern Hemisphere	47	57.5	57.5	59.2	75.8	67.7	70.3	69.7		6.2	6.2	6.6
Southern Hemisphere	15	27.2	24.3	25.7	24.2	32.0	29.7	30.3	3.8	4.7	4.7	4.3
Global	62	84.9	81.8	84.9	100	100	100	100	9.8	7.8	7.8	7.6

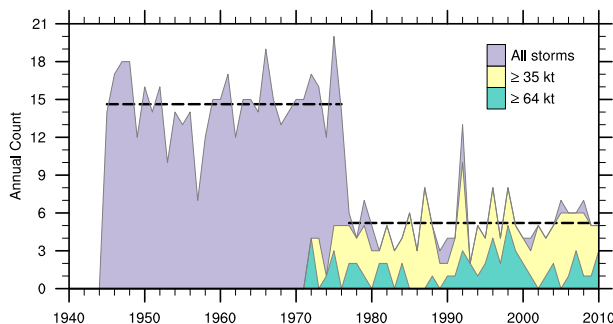


FIG. 6. Annual counts from JTWC for the north Indian region. Dashed lines identify the average number of all storms for 1945–76 (14.6) and 1977–2010 (5.2).

finds that the JTWC counts are greater at the 95% level. This paradox is probably attributable to the two outlying years, 1996 and 1998, which had four and five tropical cyclones, respectively, in the JTWC dataset (Figs. 4g, 5g).

JTWC tracks significantly more storms at all intensities in the south Indian region than RSMC La Réunion (Table 3), although the two datasets converge in the 2000s (Fig. 4h). During 2001–10, they have the same number of 35-kt storms five times, 64-kt storms five times, and 96-kt storms seven times.

The South Pacific is the only region without any significant differences in annual counts (Table 3). Meanwhile, the 64- and 96-kt thresholds in the Australian region are the only cases where JTWC has significantly fewer storms than its IBTrACS-WMO counterpart (Table 3), although the deviations are relatively modest. JTWC has more 35-kt tropical cyclones in the Australian region, but BoM has significantly more 64- and 96-kt tropical cyclones. Due in part to the offsetting differences between the south Indian and Australian regions, the total number of Southern Hemisphere storms is only significant at the 95% level for 35-kt storms.

2) COMPARISON WITH GRAY (1968) AND LANDER AND GUARD (1998)

Gray (1968) provided the first global climatology of tropical cyclone activity. This landmark study documented patterns in tropical cyclogenesis and tracks, both geographically and with respect to the annual cycle. Table 4 compares the average annual and standard deviation of the number of tropical cyclones from IBTrACS-WMO and NHC+JTWC with those from Gray (1968, his Table 1) and Lander and Guard (1998, their Table 1). Gray drew on over 50 data sources, which had periods of record ranging from 20 to 70 years depending on the region. Even so, Gray acknowledged that his data were likely to be incomplete, particularly in the east Pacific. The advent of satellite monitoring filled those

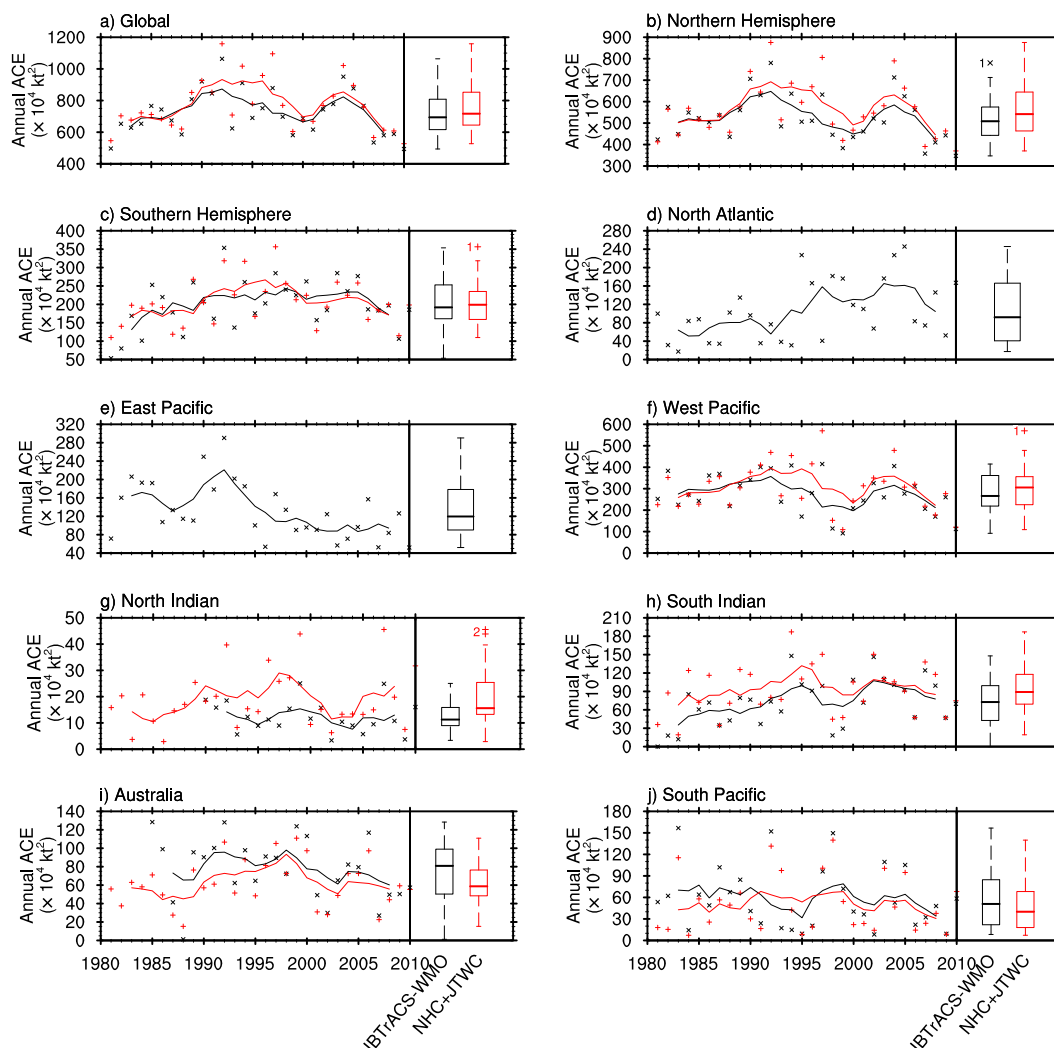


FIG. 7. Time series and box-and-whisker plots of annual ACE from IBTrACS-WMO [black lines and crisscross (\times) markers] and NHC+JTWC [red lines and cross (+) markers]. In the time series, markers identify total values, while lines show 5-yr running means.

gaps in the following decades. Gray also had somewhat different definitions for the Southern Hemisphere regions (see his Fig. 4): the Australian region was confined to the continent's northwestern coast while the northeastern coast was included in the South Pacific region. It is more accurate to compare the Southern Hemisphere as a whole rather than examining its individual regions.

Lander and Guard (1998) used a dataset similar to NHC+JTWC for the 30-yr period 1966–95. Their average annual numbers of storms are generally similar to NHC+JTWC for 1981–2010, except for the North Atlantic region, which has been exceptionally active during the recent 1995–2010 period (Fig. 4d). Lander and Guard (1998), IBTrACS-WMO, and NHC+JTWC each have more storms than Gray (1968) in every region except the north Indian.

Figure 6 illustrates that the change in the north Indian region likely relates to changing data sources in 1977. In addition to 35- and 64-kt storms, Fig. 6 shows the annual number of all storms, including those with no wind data. The average number of such storms decreased sharply from 14.6 for 1945–76 to 5.2 for 1977–2010. The average for the earlier period is close to the 13 storms per year observed by Gray (1968). JTWC's area of responsibility was expanded to the Bay of Bengal in 1971 (Chu et al. 2002). Application of the newly developed Dvorak technique to polar-orbiting satellite data explains the introduction of wind data at that time. The Arabian Sea was added in 1975. Data prior to those years come from other historical archives. However, the exact sources are unknown, and the large numbers of storms in 1971–76 are inconsistent with JTWC's

TABLE 5. As in Table 3, but for annual ACE.

Region	Source	Initial year	ACE ($\times 10^4 \text{ kt}^2$)		
			25th	50th	75th
North Atlantic	WMO: Miami	1981	41	92	166
East Pacific	WMO: Miami	1981	90	120	178
West Pacific	WMO: Tokyo	1981	219	266	361
West Pacific	JTWC	1981	225	306	356
North Indian	WMO: New Delhi	1990	9	11	16
North Indian	JTWC	1981	13	16	25
South Indian	WMO: La Réunion	1981/82	46	73	100
South Indian	JTWC	1980/81	69	89	118
Australia	WMO: BoM	1984/85	50	81	99
Australia	JTWC	1980/81	48	59	76
South Pacific	WMO: Nadi/Wellington	1980/81	22	51	85
South Pacific	JTWC	1980/81	18	40	68
Northern Hemisphere	WMO	1981	443	508	575
Northern Hemisphere	NHC+JTWC	1981	463	542	645
Southern Hemisphere	WMO	1980/81	150	210	246
Southern Hemisphere	JTWC	1980/81	162	193	233
Global	WMO	1981	616	694	808
Global	NHC+JTWC	1981	645	717	853
Global	WMO	1990	609	743	877
Global	NHC+JTWC	1990	655	769	935

annual tropical cyclone reports from that period (Chu et al. 2002). As a result of this drastic change in the north Indian region's number of storms, its contribution to the global total is reduced by more than half (from 12.9% to 4.8%–5.9%; Table 4) in the current climatology compared with Gray (1968).

Table 4 also lists the standard deviations of the annual number of storms in each region. The standard deviations of IBTrACS-WMO and NHC+JTWC are higher than those found by Lander and Guard (1998) for the North Atlantic, the east Pacific, and the Southern Hemisphere, but they are lower for west Pacific, the north Indian region, and the globe. The global standard deviation of 7.6–7.8 storms is also lower than the 8.3 storms found by Frank and Young (2007) for 1985–2003.

c. Annual accumulated cyclone energy

Bell et al. (2000) defined ACE as the sum of the squares of the 6-hourly maximum winds for all tropical cyclones with intensities of at least 35 kt. RSMC Miami has since expanded the definition to include subtropical storms (Beven et al. 2008). IBTrACS-WMO data are not always available on the standard 6-hourly synoptic times, so the ACE calculations in this study use all available data and normalize for the time between observations.

Figure 7 shows time series and box-and-whisker plots for each region, and Table 5 lists the medians and quartiles. The ACE from JTWC is significantly higher than its IBTrACS-WMO counterpart in the west Pacific,

north Indian, and south Indian regions. This relationship is reversed in the Australian and South Pacific regions. The average values for annual ACE are shown in Table 6, along with each region's fractional contribution to the global total. The values from NHC+JTWC for 1981–2010 are generally consistent with those from Maue (2011) for 1979–2010 and from Klotzbach (2006) for 1986–2005. This agreement is not surprising since both studies primarily used data from NHC and JTWC, supplemented with two of the historical archives in IBTrACS: DS824.1 from the University Corporation for Atmospheric Research (SAIC et al. 2014) and Neumann's (1999) Southern Hemisphere tracks. The largest distinction is that Klotzbach (2006) reported an average ACE for the west Pacific that is 10% greater than either NHC+JTWC or Maue (2011), but it is not clear what caused this deviation.

The time series of global ACE (Fig. 7a) shows a changing relationship between the IBTrACS-WMO and NHC+JTWC datasets. They are in good agreement during the 1980s, then diverge in the 1990s, and then begin to converge again in the 2000s. Similar variability in the west Pacific plays a major role in this global signal. Table 6 shows that the west Pacific accounts for 38%–40% of the global amount. Figure 7c shows a similar behavior in the Southern Hemisphere as well, suggesting that these differences could be related to a larger procedural change at JTWC.

One result from this analysis is that the interannual variability for global ACE is roughly double that of the

TABLE 6. As in Table 4, but for ACE.

	Avg ACE per year ($\times 10^4 \text{ kt}^2$)				Percent of global total				Std dev ($\times 10^4 \text{ kt}$)	
	Klotzbach (2006)		NHC+JTWC		Maue (2011)		Klotzbach (2006)		IBTrACS-WMO	NHC+JTWC
	Maue (2011)	Klotzbach (2006)	IBTrACS-WMO	NHC+JTWC	Maue (2011)	Klotzbach (2006)	IBTrACS-WMO	NHC+JTWC		
North Atlantic	105	110	105	105	13.8	13.5	14.3	13.7	66	66
East Pacific	127	134	132	132	16.6	16.4	18.0	17.3	61	61
West Pacific	301	340	276	305	39.4	41.6	37.6	39.9	93	109
North Indian	17	15	12	19	2.2	1.8	1.6	2.5	6	11
South Indian			74	92			10.1	12.0	36	40
Australia			77	62			10.5	8.1	33	26
South Pacific			59	50			8.0	6.5	43	39
Northern Hemisphere	550	598	525	561	72.1	73.2	71.4	73.3	107	128
Southern Hemisphere	213	217	210	204	27.9	26.6	28.6	26.7	58	55
Global	763	817	735	765	100	100	100	100	142	165

annual number of 35-kt tropical cyclones. The interquartile range for ACE in IBTrACS-WMO is $192 \times 10^4 \text{ kt}^2$, which is 28% of the median value of $694 \times 10^4 \text{ kt}^2$ (Table 5). Meanwhile, the range for 35-kt storms is 11, just 14% of the 79.5-storm median (Table 3). The percentages are similar from NHC+JTWC, or for comparing means and standard deviations (Tables 4, 6).

d. Regional variability

Figure 8 details the geographic distribution of tropical cyclone statistics using IBTrACS-WMO (left) and then shows differences with NHC+JTWC (right). These data are shown only for the 1990–2010 period when the IBTrACS-WMO has global coverage. The overall patterns resemble those found by Gray (1968) and others, since tropical cyclone activity is concentrated in the oceanic portions of intertropical convergence zones and monsoon troughs. The greatest density for tropical cyclogenesis occurs in the east Pacific (Fig. 8a), while track density peaks in the west Pacific (Fig. 8c).

Figure 8e shows the maximum intensity achieved within each grid box from 1990 to 2010. According to IBTrACS-WMO, the east Pacific and the North Atlantic are the only two regions where large areas have supported category 5 ($\geq 137 \text{ kt}$) storms. However, this pattern is likely related to the availability of aircraft reconnaissance and other differences in operational procedures. For example, the highest wind speed in the Koba et al. (1990, 1991) table is 122 kt, while the Dvorak (1984) table goes up to 170 kt. Indeed, maximum intensities from JTWC indicate widespread category 5 occurrences across the west Pacific and occasionally in the remaining regions as well (Fig. 3, Table 2). Despite having weaker maximum intensities, the west Pacific still achieves the highest concentration of ACE in the world (Fig. 8g). Apparently, the greater density of tracks near the northern Philippines (Fig. 8c) counterbalances the intensity deviations.

Differences between JTWC and the IBTrACS-WMO are shown in the right-hand column of Fig. 8. Boundaries between WMO agencies appear prominently. For example, JTWC generally has larger values of track density, maximum intensity, and ACE density than RSMC Tokyo, RSMC New Delhi, RSMC La Réunion, and RSMC Nadi. Meanwhile, BoM and RSMC Wellington have the opposite relationship with JTWC.

The contrast in track density (Fig. 8d) between JTWC and RSMC Tokyo shows a meridional gradient. JTWC tracks more storms equatorward of 20°N , while RSMC Tokyo tracks more storms farther north. A similar discrepancy between JTWC and RSMC Wellington appears in the South Pacific. These differences probably relate to procedures for storms undergoing extratropical transition.

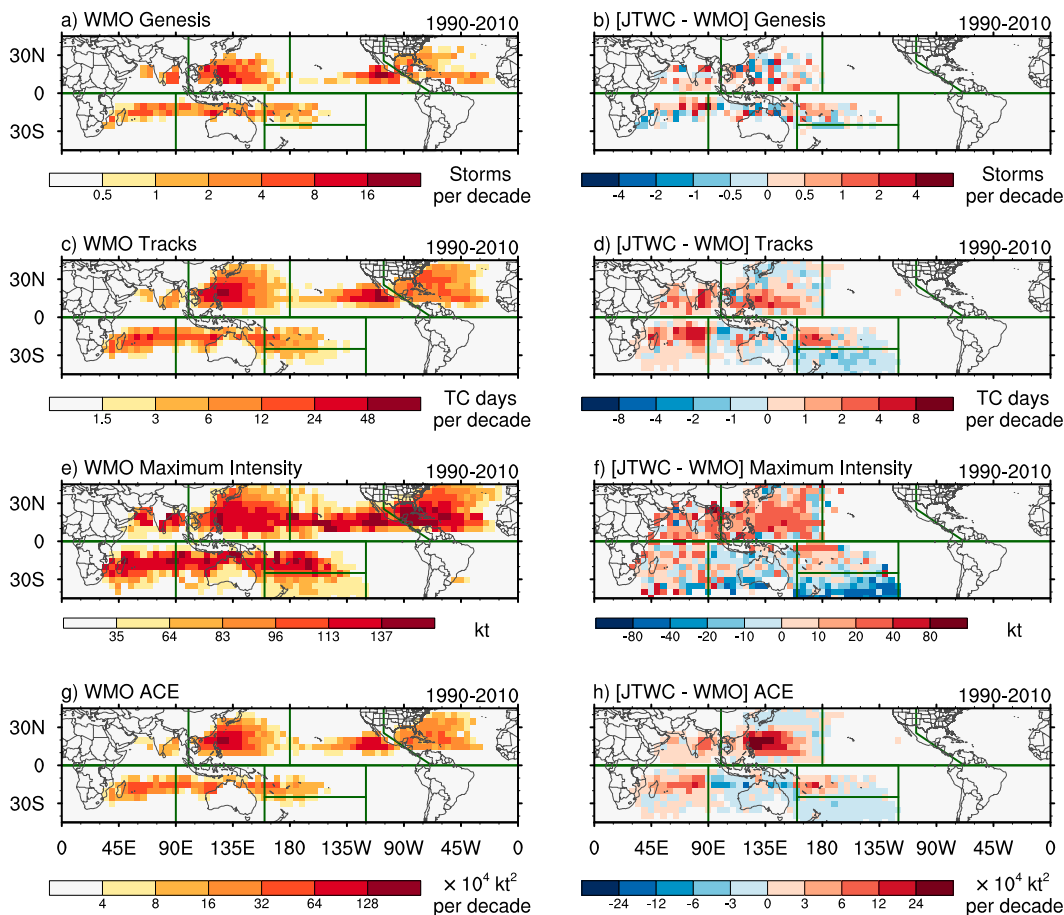


FIG. 8. Maps of accumulated tropical cyclone activity for 1990–2010 binned into $5^{\circ} \times 5^{\circ}$ grids. (left) Total values for IBTrACS-WMO and (right) the difference between NHC+JTWC and IBTrACS-WMO. (a),(b) Number of storms that first achieved 35 kt in each bin; (c),(d) track density as the number of tropical cyclone days within each bin; (e),(f) maximum tropical cyclone intensity in each bin; and (g),(h) ACE density.

e. Annual cycle

Figures 9 and 10 show the annual cycle of tropical cyclogenesis and ACE, respectively, for each region. Heavy lines show the mean, while dashed lines indicate the maximum and minimum values, excluding outliers. Consistent with Gray (1968) and others, the Northern Hemisphere regions peak in August or September, while the Southern Hemisphere regions peak between January and March. The only deviation is the north Indian region, which has two distinct maxima: pre- and postmonsoon. Most regions also show ACE lagging slightly behind tropical cyclogenesis. This may be expected as a storm can form in one month and survive long enough to contribute ACE to the following month.

The North Atlantic and South Pacific have the two shortest tropical cyclone seasons. During 1981–2010, no North Atlantic tropical cyclones formed in January–March, and only three formed in April–May (Fig. 9d).

Similarly, the South Pacific had no storms in July–September, and only one or two each in June and October (Fig. 9j). No other regions have such long and quiet off seasons.

The west Pacific has the longest and most active tropical cyclone season. All 30 years had at least one storm form in July, at least three in August, and at least two each in September and October (Fig. 9f). The only other regions and months that always produce a tropical cyclone are September in the North Atlantic and east Pacific (Figs. 9d,e). By contrast, May 1995 was the only month in the 30-yr dataset with no tropical cyclones anywhere in the globe (Fig. 9a).

6. Conclusions

The advent of IBTrACS (Knapp et al. 2010) as a collection of best track datasets facilitates comparisons between these diverse sources. This study compares the

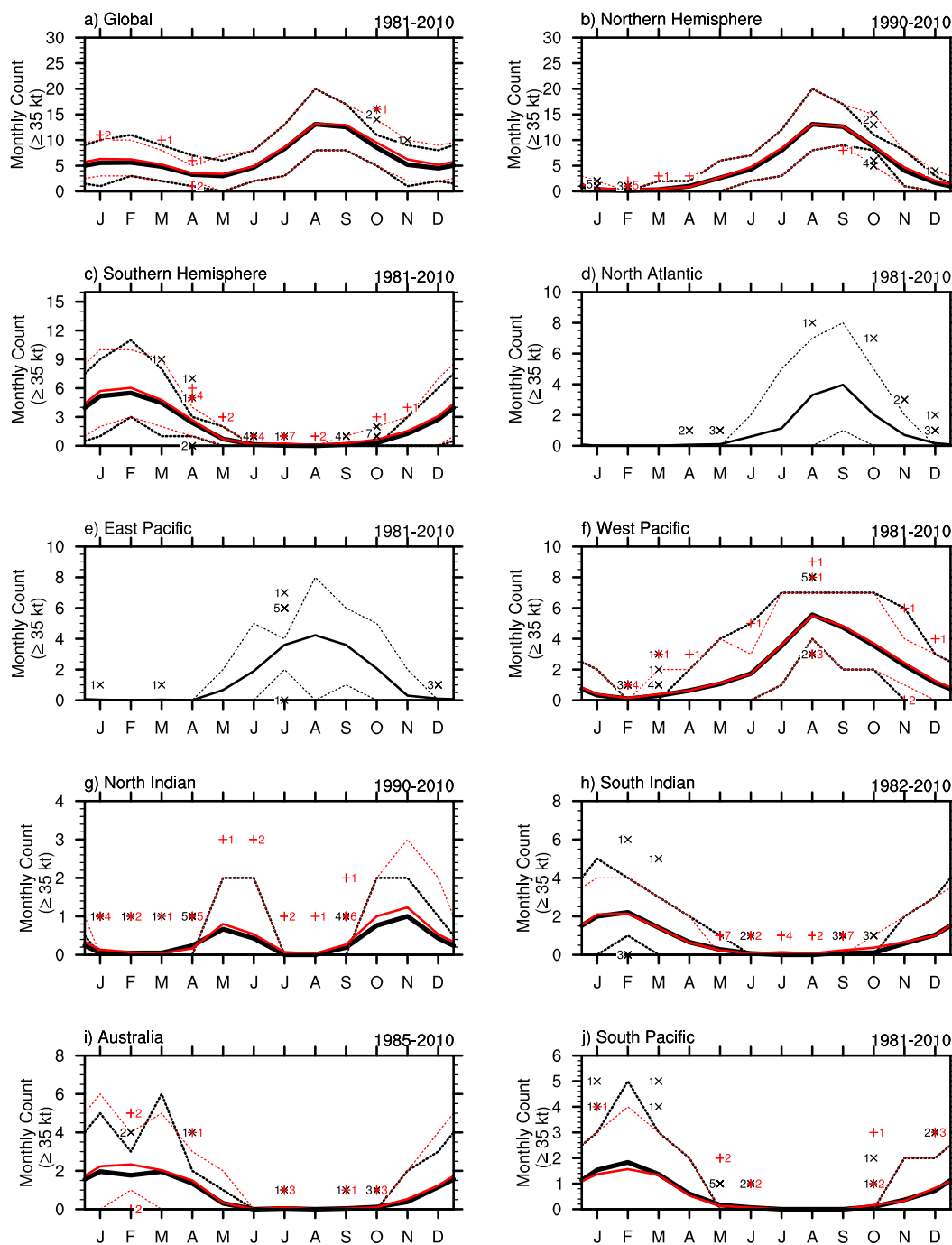


FIG. 9. Numbers of tropical cyclone formation per month in each region using IBTrACS-WMO (black) and NHC+JTWC (red). Solid lines denote the average, while dashed lines identify the maxima and minima, excluding outliers. Outliers, identified as values more than 1.5 interquartile ranges from the nearest quartile, are identified with markers. Numbers next to those markers indicate how many times that value has occurred. Years in the upper right denote the period of record for IBTrACS-WMO. NHC+JTWC is 1981–2010 for all regions.

climatology of tropical cyclones using two global datasets derived from IBTrACS: 1) the WMO subset of IBTrACS (IBTrACS-WMO) and 2) a combination of NHC for the Western Hemisphere and JTWC for the

rest of the globe (NHC+JTWC). The results illustrate how discrepancies between best track datasets can impact investigations of the global climatology of tropical cyclones.

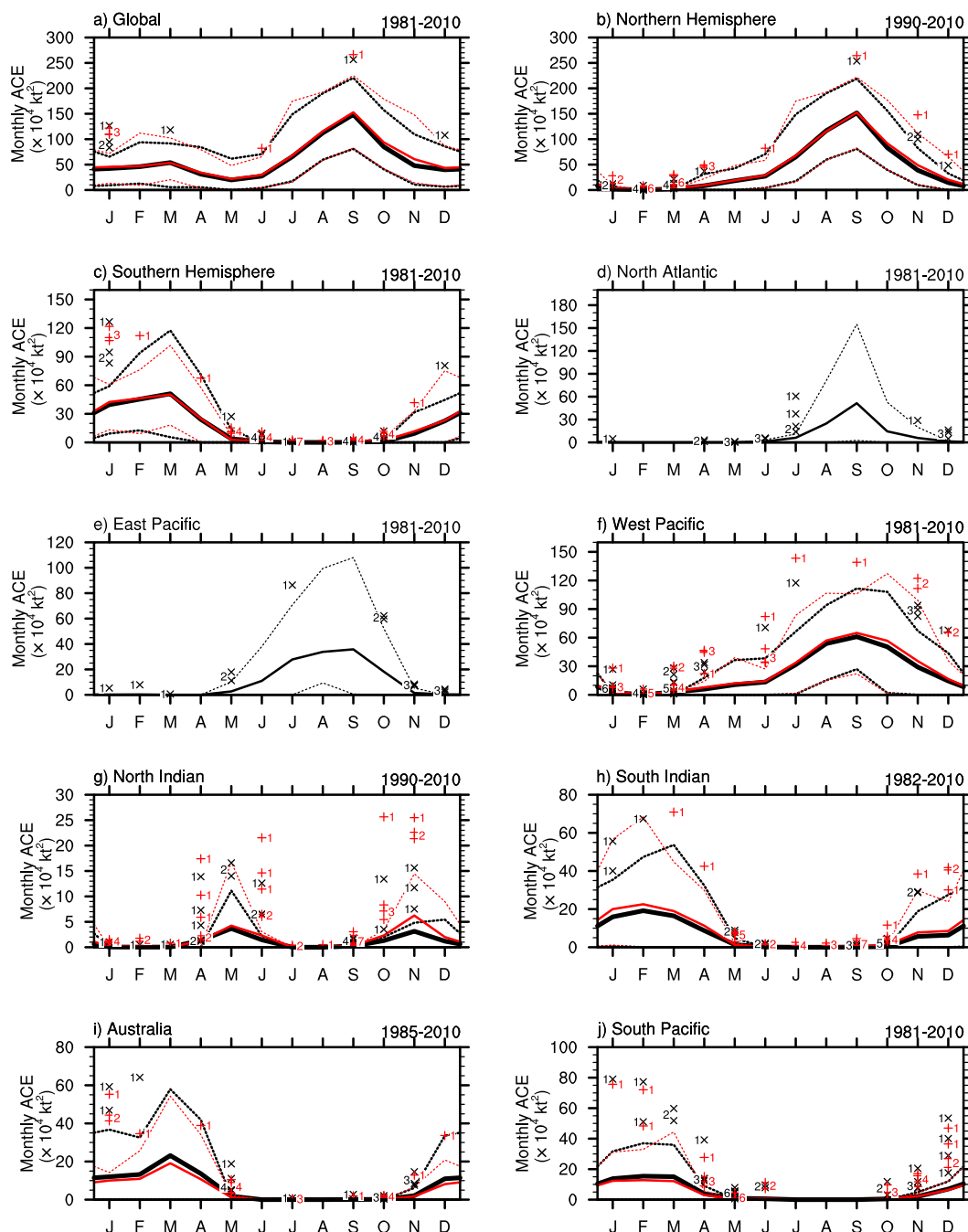


FIG. 10. As in Fig. 9, but for ACE.

IBTrACS-WMO and NHC+JTWC agree reasonably well on many key aspects of the global tropical cyclones. In both datasets, the median and upper quartile of storm LMI are near category 1 (64 kt) and category 3 (96 kt), respectively, on the Saffir–Simpson scale. This provides some physical meaning for these common thresholds. IBTrACS-WMO and NHC+JTWC also have broadly similar statistics for global annual tropical cyclone

activity. Most years from 1981 to 2010 had 74–84 storms reaching 35 kt in IBTrACS-WMO, compared with 79–90 in NHC+JTWC (Table 3). Similarly, the global annual ACE is usually $616\text{--}808 \times 10^4 \text{ kt}^2$ in IBTrACS-WMO and $645\text{--}853 \times 10^4 \text{ kt}^2$ in NHC+JTWC (Table 5). Based on these values, global ACE exhibits about twice as much interannual variability as the global number of 35-kt tropical cyclones. Finally, the geographic

and seasonal distributions of tropical cyclones are broadly similar between the datasets (Figs. 8–10).

This study also highlights some substantial differences between the IBTrACS-WMO and NHC+JTWC. The greatest disparities occur in the west Pacific, which have been documented in previous studies (Kamahori et al. 2006; Yu et al. 2007; Nakazawa and Hoshino 2009; Song et al. 2010; Knapp and Kruk 2010; Ren et al. 2011; Barcikowska et al. 2012; Knapp et al. 2013). The deviations primarily occur for stronger storms, and they become more pronounced in the 1990s (Nakazawa and Hoshino 2009; Ren et al. 2011; Barcikowska et al. 2012; Knapp et al. 2013). This study puts those contrasts into a global perspective. The west Pacific contributes 30% of the global number of tropical cyclones (Table 4) and 38%–40% of the global ACE (Table 6). The differences between JTWC and RSMC Tokyo therefore have important implications for the global climatology.

Since the termination of reconnaissance flights in the west Pacific in 1987, JTWC has used similar procedures in all regions. Their data, therefore, provide a useful benchmark for comparing other nonoverlapping agencies. For example, BoM and RSMC Tokyo have no storms in common for comparison. BoM in the Australian region has significantly more 96-kt tropical cyclones than JTWC, and RSMC Tokyo in the west Pacific has significantly fewer 96-kt storms (Table 3, Fig. 5). It therefore stands to reason that BoM's procedures may produce higher intensities than those of RSMC Tokyo. Similarly, in the South Pacific, JTWC has a larger track density than RSMC Nadi equatorward of 25°S but a smaller density than RSMC Wellington to the south (Fig. 8d). Some of this difference can be attributed to procedural distinctions between the two RSMCs. However, a similar pattern is also seen in the west Pacific, even though RSMC Tokyo covers the entire region. This similarity between regions suggests that some of the pattern in the South Pacific may also be related to JTWC procedures for handling storms that are undergoing extratropical transition.

This study highlights differences in the climatologies between NHC+JTWC and IBTrACS-WMO. Only through reanalysis can it be determined which, if either, is more accurate. Kossin et al. (2007, 2013) have shown that automated techniques can contribute to these efforts, but their skill cannot yet match that of a human analyst. Diamond et al. (2012, 2013) recently completed a reanalysis of tracks in the South Pacific, which resulted in a reduction of about one tropical cyclone per year for 1981–2010. Such reanalysis can be labor intensive, but it is underway in the south Indian (T. Dupont 2011, personal communication), east Pacific (Kimberlain 2012), and North Atlantic (Hagen et al. 2012) regions.

The challenge of manual reanalysis has also led to new innovative approaches. For example, Zhang et al. (2007) assimilated satellite data into a mesoscale model to produce a numerical reanalysis of west Pacific tropical cyclones. The process is still time-consuming, but 36 storms have been reanalyzed to date with central pressures and maximum wind speeds comparable to those found in best track datasets. Meanwhile, Hennon et al. (2014, manuscript submitted to *Bull. Amer. Meteor. Soc.*) are exploring crowdsourcing as another reanalysis method. Through a web interface, they have invited citizen scientists to answer a few questions about tropical cyclone satellite images. The responses provide an analysis similar to the original Dvorak technique. Because they draw on thousands of these citizen scientists, Hennon et al. (2014, manuscript submitted to *Bull. Amer. Meteor. Soc.*) are able to reanalyze storms in a fraction of the time it would take a trained analyst. Ultimately, however, our understanding of tropical cyclones and their relationship with climate hinges on documenting the heterogeneities in the best track dataset and rectifying them through expert reanalysis.

Acknowledgments. Paula Hennon, Michael Kruk, and Howard Diamond provided valuable inspiration for this work. We are also grateful to Ron McTaggart-Cowan, Chris Landsea, Mark Lander, and an anonymous reviewer, whose comments improved this manuscript. Schreck received support for this research from NOAA's Climate Data Record (CDR) Program through the Cooperative Institute for Climate and Satellites–North Carolina (CICS–NC).

REFERENCES

- Ayyer, A., and C. Thorncroft, 2011: Interannual-to-multidecadal variability of vertical shear and tropical cyclone activity. *J. Climate*, **24**, 2949–2962, doi:10.1175/2010JCLI3698.1.
- Applequist, S., A. Arguez, I. Durre, M. F. Squires, R. S. Vose, and X. Yin, 2012: 1981–2010 U.S. hourly normals. *Bull. Amer. Meteor. Soc.*, **93**, 1637–1640, doi:10.1175/BAMS-D-11-00173.1.
- Arguez, A., and R. S. Vose, 2011: The definition of the standard WMO climate normal: The key to deriving alternative climate normals. *Bull. Amer. Meteor. Soc.*, **92**, 699–704, doi:10.1175/2010BAMS2955.1.
- , I. Durre, S. Applequist, R. S. Vose, M. F. Squires, X. Yin, R. R. Heim, and T. W. Owen, 2012: NOAA's 1981–2010 U.S. climate normals: An overview. *Bull. Amer. Meteor. Soc.*, **93**, 1687–1697, doi:10.1175/BAMS-D-11-00197.1.
- , R. S. Vose, and J. Dissen, 2013: Alternative climate normals: Impacts to the energy industry. *Bull. Amer. Meteor. Soc.*, **94**, 915–917, doi:10.1175/BAMS-D-12-00155.1.
- Avila, L. A., and S. R. Stewart, 2013: Atlantic hurricane season of 2011. *Mon. Wea. Rev.*, **141**, 2577–2596, doi:10.1175/MWR-D-12-00230.1.
- Barcikowska, M., F. Feser, and H. von Storch, 2012: Usability of best track data in climate statistics in the western North

- Pacific. *Mon. Wea. Rev.*, **140**, 2818–2830, doi:[10.1175/MWR-D-11-00175.1](https://doi.org/10.1175/MWR-D-11-00175.1).
- Bell, G. D., and Coauthors, 2000: The 1999 North Atlantic and eastern North Pacific hurricane seasons [in “Climate Assessment for 1999”]. *Bull. Amer. Meteor. Soc.*, **81** (6), S19–S22, doi:[10.1175/1520-0477\(2000\)81\[s1:CAF\]2.0.CO;2](https://doi.org/10.1175/1520-0477(2000)81[s1:CAF]2.0.CO;2).
- Beven, J. L., and Coauthors, 2008: Atlantic hurricane season of 2005. *Mon. Wea. Rev.*, **136**, 1109–1173, doi:[10.1175/2007MWR2074.1](https://doi.org/10.1175/2007MWR2074.1).
- Blake, E. S., and T. B. Kimberlain, 2013: Eastern North Pacific hurricane season of 2011. *Mon. Wea. Rev.*, **141**, 1397–1412, doi:[10.1175/MWR-D-12-00192.1](https://doi.org/10.1175/MWR-D-12-00192.1).
- Christensen, J. H., and Coauthors, 2014: Climate phenomena and their relevance for future regional climate change. *Climate Change 2013: The Physical Science Basis*, T. F. Stocker et al., Eds., Cambridge University Press, 1217–1308.
- Chu, J.-H., C. R. Sampson, A. S. Levine, and E. Fukada, 2002: The joint typhoon warning center tropical cyclone best-tracks, 1945–2000. Naval Research Laboratory Rep. NRL/MR/7540-02-16, 22 pp.
- Diamond, H. J., Ed., 2013: The tropics [in “State of the Climate in 2012”]. *Bull. Amer. Meteor. Soc.*, **94** (8), S79–S108, doi:[10.1175/2013BAMSStateoftheClimate.1](https://doi.org/10.1175/2013BAMSStateoftheClimate.1).
- , A. M. Lorrey, K. R. Knapp, and D. H. Levinson, 2012: Development of an enhanced tropical cyclone tracks database for the southwest Pacific from 1840 to 2010. *Int. J. Climatol.*, **32**, 2240–2250, doi:[10.1002/joc.2412](https://doi.org/10.1002/joc.2412).
- , —, and J. A. Renwick, 2013: A southwest Pacific tropical cyclone climatology and linkages to the El Niño–Southern Oscillation. *J. Climate*, **26**, 3–25, doi:[10.1175/JCLI-D-12-00077.1](https://doi.org/10.1175/JCLI-D-12-00077.1).
- Durre, I., M. F. Squires, R. S. Vose, X. Yin, A. Arguez, and S. Applequist, 2013: NOAA’s 1981–2010 U.S. climate normals: Monthly precipitation, snowfall, and snow depth. *J. Appl. Meteor. Climatol.*, **52**, 2377–2395, doi:[10.1175/JAMC-D-13-051.1](https://doi.org/10.1175/JAMC-D-13-051.1).
- Dvorak, V. F., 1972: A technique for the analysis and forecasting of tropical cyclone intensities from satellite pictures. NOAA Tech. Rep. NESS 36, 15 pp.
- , 1973: A technique for the analysis and forecasting of tropical cyclone intensities from satellite pictures (revision of NESS 36). NOAA Tech. Rep. NESS 45, 19 pp.
- , 1975: Tropical cyclone intensity analysis and forecasting from satellite imagery. *Mon. Wea. Rev.*, **103**, 420–430, doi:[10.1175/1520-0493\(1975\)103<0420:TCIAAF>2.0.CO;2](https://doi.org/10.1175/1520-0493(1975)103<0420:TCIAAF>2.0.CO;2).
- , 1984: Tropical cyclone intensity analysis using satellite data. NOAA Tech. Rep. NESDIS 11, 50 pp. [Available online at ftp://satapsanone.nesdis.noaa.gov/Publications/Tropical/Dvorak_1984.pdf.]
- Emanuel, K., 2005: Increasing destructiveness of tropical cyclones over the past 30 years. *Nature*, **436**, 686–688, doi:[10.1038/nature03906](https://doi.org/10.1038/nature03906).
- Frank, W. M., and G. S. Young, 2007: The interannual variability of tropical cyclones. *Mon. Wea. Rev.*, **135**, 3587–3598, doi:[10.1175/MWR3435.1](https://doi.org/10.1175/MWR3435.1).
- Gray, W. M., 1968: Global view of the origin of tropical disturbances and storms. *Mon. Wea. Rev.*, **96**, 669–700, doi:[10.1175/1520-0493\(1968\)096<0669:GVOTOO>2.0.CO;2](https://doi.org/10.1175/1520-0493(1968)096<0669:GVOTOO>2.0.CO;2).
- Hagen, A. B., and C. W. Landsea, 2012: On the classification of extreme Atlantic hurricanes utilizing mid-twentieth-century monitoring capabilities. *J. Climate*, **25**, 4461–4475, doi:[10.1175/JCLI-D-11-00420.1](https://doi.org/10.1175/JCLI-D-11-00420.1).
- , D. Strahan-Sakoskie, and C. Lockett, 2012: A reanalysis of the 1944–53 Atlantic hurricane seasons—The first decade of aircraft reconnaissance. *J. Climate*, **25**, 4441–4460, doi:[10.1175/JCLI-D-11-00419.1](https://doi.org/10.1175/JCLI-D-11-00419.1).
- Harper, B. A., J. Kepert, and J. Ginger, 2010: Guidelines for converting between various wind averaging periods in tropical cyclone conditions. WMO/TD 1555, World Meteorological Organization, 54 pp. [Available online at www.wmo.int/pages/prog/www/tcp/documents/WMO_TD_1555_en.pdf.]
- Hartmann, D. L., and Coauthors, 2014: Observations: Atmosphere and surface. *Climate Change 2013: The Physical Science Basis*, T. F. Stocker et al., Eds., Cambridge University Press, 159–254.
- Kamahori, H., N. Yamazaki, N. Mannoji, and K. Takahashi, 2006: Variability in intense tropical cyclone days in the western North Pacific. *SOLA*, **2**, 104–107, doi:[10.2151/sola.2006-027](https://doi.org/10.2151/sola.2006-027).
- Kimberlain, T. B., 2012: Re-analysis of the eastern North Pacific HURDAT. *30th Conf. on Hurricanes and Tropical Meteorology*, Ponte Vedra Beach, FL, Amer. Meteor. Soc., 2B.2. [Available online at <https://ams.confex.com/ams/30Hurricane/webprogram/Paper204625.html>.]
- Klotzbach, P. J., 2006: Trends in global tropical cyclone activity over the past twenty years (1986–2005). *Geophys. Res. Lett.*, **33**, L10805, doi:[10.1029/2006GL025881](https://doi.org/10.1029/2006GL025881).
- Knaff, J. A., D. P. Brown, J. Courtney, G. M. Gallina, and J. L. Beven, 2010: An evaluation of Dvorak technique-based tropical cyclone intensity estimates. *Wea. Forecasting*, **25**, 1362–1379, doi:[10.1175/2010WAF2222375.1](https://doi.org/10.1175/2010WAF2222375.1).
- Knapp, K. R., and M. C. Kruk, 2010: Quantifying interagency differences in tropical cyclone best-track wind speed estimates. *Mon. Wea. Rev.*, **138**, 1459–1473, doi:[10.1175/2009MWR3123.1](https://doi.org/10.1175/2009MWR3123.1).
- , —, D. H. Levinson, H. J. Diamond, and C. J. Neumann, 2010: The International Best Track Archive for Climate Stewardship (IBTrACS). *Bull. Amer. Meteor. Soc.*, **91**, 363–376, doi:[10.1175/2009BAMS2755.1](https://doi.org/10.1175/2009BAMS2755.1).
- , and Coauthors, 2011: Globally gridded satellite observations for climate studies. *Bull. Amer. Meteor. Soc.*, **92**, 893–907, doi:[10.1175/2011BAMS3039.1](https://doi.org/10.1175/2011BAMS3039.1).
- , J. A. Knaff, C. R. Sampson, G. M. Riggio, and A. D. Schnapp, 2013: A pressure-based analysis of the historical western North Pacific tropical cyclone intensity record. *Mon. Wea. Rev.*, **141**, 2611–2631, doi:[10.1175/MWR-D-12-00323.1](https://doi.org/10.1175/MWR-D-12-00323.1).
- Knutson, T. R., and Coauthors, 2010: Tropical cyclones and climate change. *Nat. Geosci.*, **3**, 157–163, doi:[10.1038/ngeo779](https://doi.org/10.1038/ngeo779).
- Koba, H., S. Osano, T. Hagiwara, S. Akashi, and T. Kikuchi, 1989: An evaluation of the rule of CI number determination in Dvorak technique for tropical cyclone crossing the Philippine Islands (in Japanese). *J. Meteor. Res.*, **41**, 157–163.
- , T. Hagiwara, S. Osano, and S. Akashi, 1990: Relationship between CI number Dvorak’s technique and minimum sea level pressure or maximum wind speed of tropical cyclone (in Japanese). *J. Meteor. Res.*, **42**, 59–67.
- , —, —, and —, 1991: Relationships between CI number and minimum sea level pressure/maximum wind speed of tropical cyclones. *Geophys. Mag.*, **44**, 15–25.
- Kossin, J. P., and D. J. Vimont, 2007: A more general framework for understanding Atlantic hurricane variability and trends. *Bull. Amer. Meteor. Soc.*, **88**, 1767–1781, doi:[10.1175/BAMS-88-11-1767](https://doi.org/10.1175/BAMS-88-11-1767).
- , K. R. Knapp, D. J. Vimont, R. J. Murnane, and B. A. Harper, 2007: A globally consistent reanalysis of hurricane variability and trends. *Geophys. Res. Lett.*, **34**, L04815, doi:[10.1029/2006GL028836](https://doi.org/10.1029/2006GL028836).

- , S. J. Camargo, and M. Sitkowski, 2010: Climate modulation of North Atlantic hurricane tracks. *J. Climate*, **23**, 3057–3076, doi:[10.1175/2010JCLI3497.1](https://doi.org/10.1175/2010JCLI3497.1).
- , T. L. Olander, and K. R. Knapp, 2013: Trend analysis with a new global record of tropical cyclone intensity. *J. Climate*, **26**, 9960–9976, doi:[10.1175/JCLI-D-13-00262.1](https://doi.org/10.1175/JCLI-D-13-00262.1).
- Lander, M. A., and C. P. Guard, 1998: A look at global tropical cyclone activity during 1995: Contrasting high Atlantic activity with low activity in other basins. *Mon. Wea. Rev.*, **126**, 1163–1173, doi:[10.1175/1520-0493\(1998\)126<1163:ALAGTC>2.0.CO;2](https://doi.org/10.1175/1520-0493(1998)126<1163:ALAGTC>2.0.CO;2).
- Landsea, C. W., 2007: Counting Atlantic tropical cyclones back to 1900. *Eos, Trans. Amer. Geophys. Union*, **88**, 197–202, doi:[10.1029/2007EO180001](https://doi.org/10.1029/2007EO180001).
- , and J. L. Franklin, 2013: Atlantic Hurricane database uncertainty and presentation of a new database format. *Mon. Wea. Rev.*, **141**, 3576–3592, doi:[10.1175/MWR-D-12-00254.1](https://doi.org/10.1175/MWR-D-12-00254.1).
- , B. A. Harper, K. Hoarau, and J. A. Knaff, 2006: Can we detect trends in extreme tropical cyclones? *Science*, **313**, 452–454, doi:[10.1126/science.1128448](https://doi.org/10.1126/science.1128448).
- , G. A. Vecchi, L. Bengtsson, and T. R. Knutson, 2010: Impact of duration thresholds on Atlantic tropical cyclone counts. *J. Climate*, **23**, 2508–2519, doi:[10.1175/2009JCLI3034.1](https://doi.org/10.1175/2009JCLI3034.1).
- Levinson, D. H., H. J. Diamond, K. R. Knapp, M. C. Kruk, and E. J. Gibney, 2010: Toward a homogenous global tropical cyclone best-track dataset. *Bull. Amer. Meteor. Soc.*, **91**, 377–380, doi:[10.1175/2010BAMS2930.1](https://doi.org/10.1175/2010BAMS2930.1).
- Mann, M. E., T. A. Sabbatelli, and U. Neu, 2007: Evidence for a modest undercount bias in early historical Atlantic tropical cyclone counts. *Geophys. Res. Lett.*, **34**, L22707, doi:[10.1029/2007GL031781](https://doi.org/10.1029/2007GL031781).
- Maue, R. N., 2009: Northern Hemisphere tropical cyclone activity. *Geophys. Res. Lett.*, **36**, L05805, doi:[10.1029/2008GL035946](https://doi.org/10.1029/2008GL035946).
- , 2011: Recent historically low global tropical cyclone activity. *Geophys. Res. Lett.*, **38**, L14803, doi:[10.1029/2011GL047711](https://doi.org/10.1029/2011GL047711).
- Nakazawa, T., and S. Hoshino, 2009: Intercomparison of Dvorak parameters in the tropical cyclone datasets over the western North Pacific. *SOLA*, **5**, 33–36, doi:[10.2151/sola.2009-009](https://doi.org/10.2151/sola.2009-009).
- Neumann, C. J., 1999: The HURISK model: An adaptation for the Southern Hemisphere (A user's manual). Science Applications International Corporation, Monterey, CA, 31 pp.
- Pielke, R. A., Jr., C. Landsea, M. Mayfield, J. Laver, and R. Pasch, 2005: Hurricanes and global warming. *Bull. Amer. Meteor. Soc.*, **86**, 1571–1575, doi:[10.1175/BAMS-86-11-1571](https://doi.org/10.1175/BAMS-86-11-1571).
- Rappaport, E. N., 2000: Loss of life in the United States associated with recent Atlantic tropical cyclones. *Bull. Amer. Meteor. Soc.*, **81**, 2065–2073, doi:[10.1175/1520-0477\(2000\)081<2065:LOLITU>2.3.CO;2](https://doi.org/10.1175/1520-0477(2000)081<2065:LOLITU>2.3.CO;2).
- Ren, F., J. Liang, G. Wu, W. Dong, and X. Yang, 2011: Reliability analysis of climate change of tropical cyclone activity over the western North Pacific. *J. Climate*, **24**, 5887–5898, doi:[10.1175/2011JCLI3996.1](https://doi.org/10.1175/2011JCLI3996.1).
- Saffir, H. S., 1973: Hurricane wind and storm surge. *Mil. Eng.*, **423**, 4–5.
- SAIC, NHC, JTWC, UCAR/NCAR, and BoM, cited 2014: Global tropical cyclone “best track” position and intensity data. Dataset ds824.1, CISL Research Data Archive, National Center for Atmospheric Research, Boulder, CO. [Available online at <http://rda.ucar.edu/datasets/ds824.1/>.]
- Schott, T., and Coauthors, 2012: The Saffir–Simpson hurricane wind scale. National Weather Service Doc., 4 pp. [Available online www.nhc.noaa.gov/pdf/sshs.pdf.]
- Seneviratne, S. I., and Coauthors, 2012: Changes in climate extremes and their impacts on the natural physical environment. *Managing the Risks of Extreme Events and Disasters to Advance Climate Change Adaptation*, C. B. Field et al., Eds., Cambridge University Press, 109–230.
- Simpson, R. H., 1974: The hurricane disaster—Potential scale. *Weatherwise*, **27**, 169–186, doi:[10.1080/00431672.1974.9931702](https://doi.org/10.1080/00431672.1974.9931702).
- Smith, A. B., and R. W. Katz, 2013: US billion-dollar weather and climate disasters: Data sources, trends, accuracy and biases. *Nat. Hazards*, **67**, 387–410, doi:[10.1007/s11069-013-0566-5](https://doi.org/10.1007/s11069-013-0566-5).
- Song, J.-J., Y. Wang, and L. Wu, 2010: Trend discrepancies among three best track data sets of western North Pacific tropical cyclones. *J. Geophys. Res.*, **115**, D12128, doi:[10.1029/2009JD013058](https://doi.org/10.1029/2009JD013058).
- Torn, R. D., and C. Snyder, 2012: Uncertainty of tropical cyclone best-track information. *Wea. Forecasting*, **27**, 715–729, doi:[10.1175/WAF-D-11-00085.1](https://doi.org/10.1175/WAF-D-11-00085.1).
- Vecchi, G. A., and T. R. Knutson, 2008: On estimates of historical North Atlantic tropical cyclone activity. *J. Climate*, **21**, 3580–3600, doi:[10.1175/2008JCLI2178.1](https://doi.org/10.1175/2008JCLI2178.1).
- Velden, C., and Coauthors, 2006a: The Dvorak tropical cyclone intensity estimation technique: A satellite-based method that has endured for over 30 years. *Bull. Amer. Meteor. Soc.*, **87**, 1195–1210, doi:[10.1175/BAMS-87-9-1195](https://doi.org/10.1175/BAMS-87-9-1195).
- , and Coauthors, 2006b: Supplement to: The Dvorak tropical cyclone intensity estimation technique: A satellite-based method that has endured for over 30 years. *Bull. Amer. Meteor. Soc.*, **87**, S6–S9, doi:[10.1175/BAMS-87-9-Velden](https://doi.org/10.1175/BAMS-87-9-Velden).
- Villarini, G., G. A. Vecchi, T. R. Knutson, M. Zhao, and J. A. Smith, 2011: North Atlantic tropical storm frequency response to anthropogenic forcing: Projections and sources of uncertainty. *J. Climate*, **24**, 3224–3238, doi:[10.1175/2011JCLI3853.1](https://doi.org/10.1175/2011JCLI3853.1).
- Webster, P. J., 2008: Myanmar's deadly daffodil. *Nat. Geosci.*, **1**, 488–490, doi:[10.1038/ngeo257](https://doi.org/10.1038/ngeo257).
- , G. J. Holland, J. A. Curry, and H.-R. Chang, 2005: Changes in tropical cyclone number, duration, and intensity in a warming environment. *Science*, **309**, 1844–1846, doi:[10.1126/science.1116448](https://doi.org/10.1126/science.1116448).
- Wilks, D. S., 2006: *Statistical Methods in the Atmospheric Sciences*. 2nd ed. Academic Press, 627 pp.
- Wu, M.-C., K.-H. Yeung, and W.-L. Chang, 2006: Trends in western North Pacific tropical cyclone intensity. *Eos, Trans. Amer. Geophys. Union*, **87**, 537–538, doi:[10.1029/2006EO480001](https://doi.org/10.1029/2006EO480001).
- Yu, H., C. Hu, and L. Jiang, 2007: Comparison of three tropical cyclone intensity datasets. *Acta Meteor. Sin.*, **21**, 121–128.
- Zhang, X., T. Li, F. Weng, C.-C. Wu, and L. Xu, 2007: Reanalysis of western Pacific typhoons in 2004 with multi-satellite observations. *Meteor. Atmos. Phys.*, **97**, 3–18, doi:[10.1007/s00703-006-0240-5](https://doi.org/10.1007/s00703-006-0240-5).